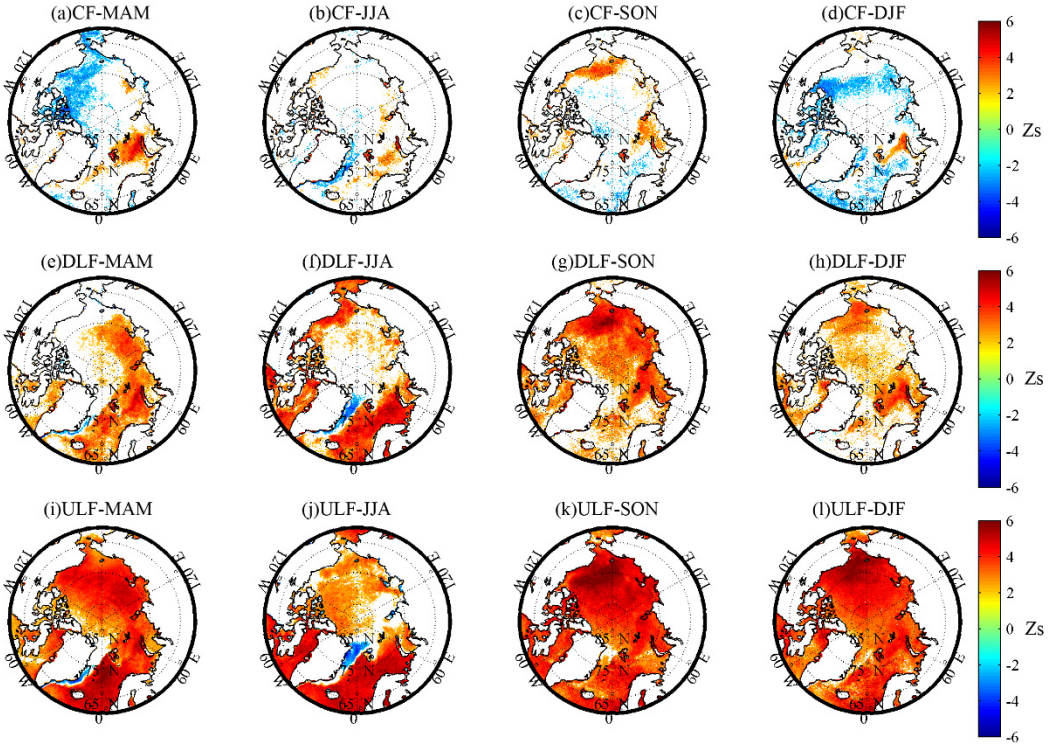

Figure S1. Spatial distributions of Zs derived by the Mann-Kendall test over the seas in Arctic (60°N~90°N) for different seasons from 1982 to 2019 at 14:00 LST. (**a**–**d**) CF in MAM, JJA, SON, and DJF. (**e**–**h**) DLF in MAM, JJA, SON, and DJF. (**i**–**l**) ULF in MAM, JJA, SON, and DJF. The colored regions are at a significance level of 95%.

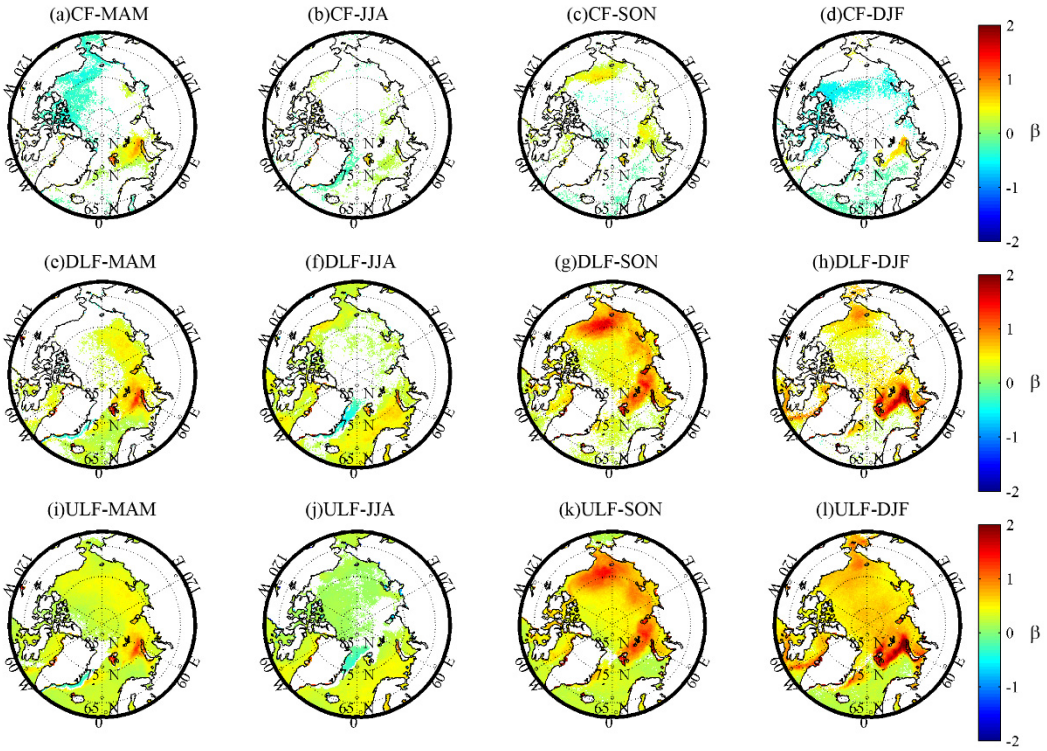

Figure S2. Spatial distributions of β derived by the Sen's slope test over the seas in Arctic (60°~90° N) for different seasons from 1982 to 2019 at 14:00 LST. (**a**–**d**) CF in MAM, JJA, SON, and DJF. (**e**–**h**) DLF in MAM, JJA, SON, and DJF. (**i**–**l**) ULF in MAM, JJA, SON, and DJF. The colored regions are at a significance level of 95%.

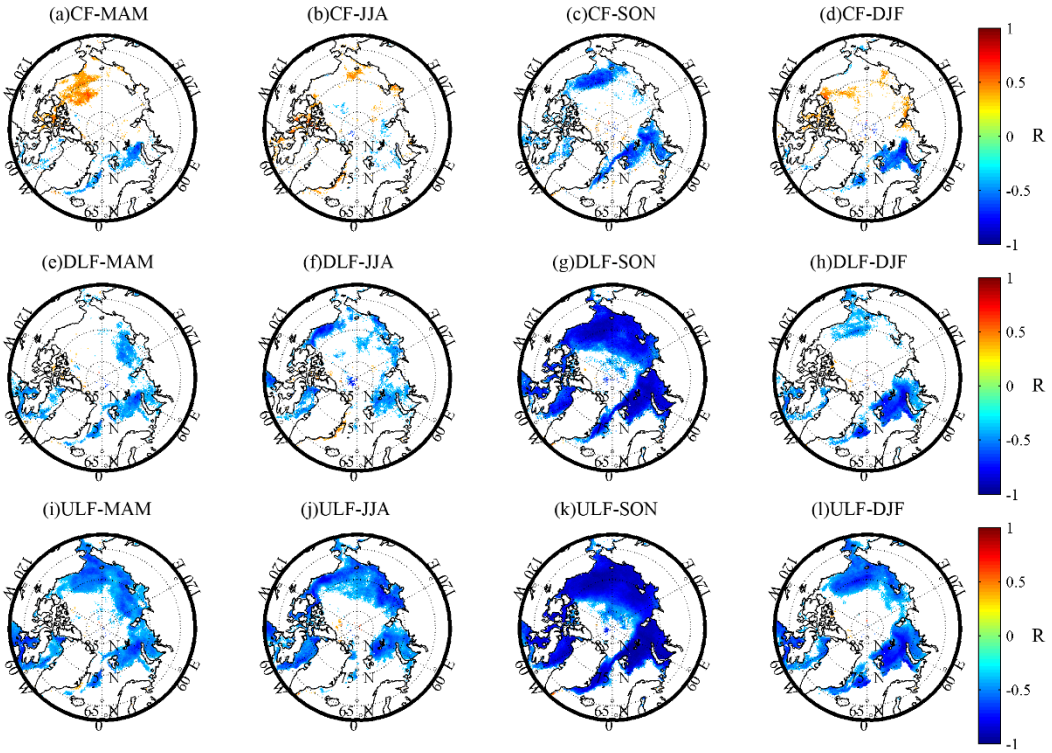

Figure S3. Seasonal distributions of Pearson's correlation coefficient R (with $p < 0.05$) between the autumn SIC and (**a**–**d**) CF, (**e**–**h**) DLF, (**i**–**l**) ULF over the seas in Arctic (60°N~90°N) from 1987 to 2019 at 14:00 LST. (**a**,**e**,**i**) MAM; (**b**,**f**,**j**) JJA; (**c**,**g**,**k**) SON; (**d**,**h**,**l**) DJF.